





AKADÉMIAI KIADÓ

MYC integrates FSH signalling networks in cumulus cells during bovine oocyte maturation

LUDYMILA F. CANTANHÊDE¹, MARCELO T. MOURA^{1*} ,
ROBERTA L. OLIVEIRA-SILVA² , PÁBOLA S. NASCIMENTO¹,
JOSÉ C. FERREIRA-SILVA¹, ANA M. BENKO-ISEPPON² and
MARCOS A. L. OLIVEIRA¹

Acta Veterinaria
Hungarica

70 (2022) 2, 132–142

DOI:
10.1556/004.2022.00007
© 2022 Akadémiai Kiadó, Budapest

¹ Departamento de Medicina Veterinária, Universidade Federal Rural de Pernambuco – UFRPE, Recife, Brazil

² Departamento de Genética, Universidade Federal de Pernambuco – UFPE, Recife, Brazil

Received: 13 August 2021 • Accepted: 24 March 2022
Published online: 2 May 2022

RESEARCH ARTICLE



ABSTRACT

Follicle-stimulating hormone (FSH) contributes to the acquisition of oocyte competence by modulating signalling pathways in cumulus cells (CCs), albeit much less is known about transcription factors (TFs) that orchestrate the downstream transcriptional changes. This work allowed to prospect TFs involved in FSH-mediated signalling during oocyte *in vitro* maturation (IVM). Bovine cumulus-oocyte complexes underwent IVM with FSH (FSH+) or without FSH (control/CTL) for 22 h, and CCs were subjected to gene expression profiling. Five software identified reference genes for RT-qPCR (ATP1A1, UBB, and YWHAZ). The transcript levels of FSH-responsive genes HAS2 and PTGS2 (COX2) validated the experimental design. Among candidate TFs, MYC was down-regulated (0.35-fold; $P < 0.0001$), and THAP11 (RONIN) was up-regulated (1.47-fold; $P = 0.016$) under FSH+ conditions. *In silico* analyses predicted binding motifs at MYC and THAP11 genes for previously known FSH-responsive TFs. Signalling pathways (EGFR, ERK, GSK3, PKA, and P38) may execute post-translational regulation due to potential phosphorylation sites in MYC and THAP11 proteins. Prediction of protein-protein interaction networks showed MYC as a core component of FSH signalling, albeit THAP11 acts independently. Hence, MYC integrates FSH signalling networks and may assist in exploring genome-wide transcriptional changes associated with the acquisition of oocyte competence.

KEYWORDS

Bos taurus, gonadotropin, granulosa, housekeeping genes, *RONIN*

INTRODUCTION

Oocyte maturation and acquisition of developmental competence (*i.e.*, capacity to be fertilised and sustain full-term development) are complex processes that require the interplay of multiple cell types (Russell et al., 2016; Andrade et al., 2019). This crosstalk between the somatic compartment (theca, mural granulosa, and cumulus cells – CCs) and the follicle-enclosed oocyte is paramount for its growth and maturation. There is intense bidirectional paracrine signalling among these cell types, with the exchange of ions, growth factors, hormones, small vesicle particles (exosomes), and RNAs (Macaulay et al., 2016; Russell et al., 2016). There is also endocrine signalling, where gonadotropins (follicle-stimulating hormone – FSH and luteinising hormone – LH) produced in the pituitary travel through the bloodstream to act upon follicular somatic cells (Russell et al., 2016). This crosstalk modulates critical developmental processes such as folliculogenesis, resumption of meiosis, oocyte metabolism, and the acquisition of developmental competence (Russell et al., 2016; Andrade et al., 2019).

The CCs mediate FSH signalling since oocytes lack FSH receptors (FSHR) (Nuttinck et al., 2004; Lonergan and Fair, 2016). Several studies have shown that FSH is dispensable

*Corresponding author.
E-mail: marcelotmoura@gmail.com



for the resumption of meiosis and oocyte nuclear maturation (Sirard et al., 2007), albeit necessary for oocyte cytoplasm maturation and the acquisition of developmental competence (Sirard et al., 2007; Assidi et al., 2013; Lonergan and Fair, 2016). Gonadotropin binding to FSHR triggers downstream signalling pathways such as cAMP-dependent protein kinase A (PKA), phosphatidylinositol-4,5-bisphosphate 3-kinases (PI3K)/protein kinase B (PKB/AKT), extracellular-regulated kinases (ERK1/2), and P38 mitogen-activated protein kinase (P38) (Gloaguen et al., 2011; Casarini and Crépieux, 2019). FSH alongside Epidermal Growth Factor (EGF) ligands promotes EGR receptor (EGFR) mediated ERK1/2, PKB/AKT, and Janus kinase/signal transducers and activators of transcription (JAK/STAT) signalling (Gloaguen et al., 2011; Richani and Gilchrist, 2018). These complex pathway interactions during oocyte growth and maturation elicit substantial transcriptional changes in the oocyte and CCs (Blaha et al., 2015; Khan et al., 2015). Transcription factors (TFs) act downstream of these signalling pathways (e.g., CREB, FOXL2, FOXO1) and mediate the transcriptional changes (Gloaguen et al., 2011; Kuo et al., 2012; Herndon et al., 2016; Casarini and Crépieux, 2019). There are likely other yet unknown TFs participating in this process. Finding additional TFs downstream FSH signalling should substantially contribute to understanding oocyte maturation and the acquisition of developmental competence.

Accurate gene expression analysis may assist in identifying TFs that co-ordinate transcriptional changes downstream FSH signalling pathways. Reverse transcription quantitative PCR (RT-qPCR) is a standard tool for gene expression profiling. Several factors may hinder the accuracy of RT-qPCR assays, such as fluctuations in RNA integrity, inter-sample variation (Taylor et al., 2019). Reference genes (RGs) allow accurate RT-qPCR by counterbalancing potential bias from both experimental and technical factors (Chapman and Waldenström, 2015; Taylor et al., 2019). A previous study used three RGs and the GeNorm software for RT-qPCR normalisation under varying FSH conditions (Khan et al., 2015), albeit it did not describe the stability values of such RGs. To the best of our knowledge, no report screened several candidate RGs and applied multiple software to select the most stable RGs under such conditions.

This work aimed to design an accurate RT-qPCR assay with validated RGs and prospect TFs involved in mediating FSH signalling during bovine oocyte maturation. The prediction of TF integration into FSH signalling networks relied on DNA-binding motifs, post-translational modifications, and protein-protein interaction networks.

MATERIALS AND METHODS

Ethics statement

The Ethics Committee (CEUA) at the Federal Rural University of Pernambuco (UFRPE) approved the project under license 030/2016.

Ovary collection and *in vitro* maturation (IVM)

These procedures were carried out as described by Cantanhêde et al. (2021). Ovaries were collected at a local slaughterhouse (Caruaru, Pernambuco, Brazil) and transported in saline solution (0.9% NaCl) containing 10 µg mL⁻¹ penicillin and streptomycin (Gibco) at 35 °C. The cumulus-oocyte complexes (COCs) were retrieved from 2 to 8 mm follicles in TCM-199 medium with Hank's salts (Sigma Aldrich) supplemented with 2.0 mM L-glutamine (Sigma Aldrich), 10% fetal bovine serum (FBS; Gibco) and 0.05 mg mL⁻¹ gentamicin sulphate (Gibco). COCs were selected based on at least three layers of CCs and an evenly granulated oocyte cytoplasm (Moura et al., 2018). IVM medium was formulated with TCM-199 with Earle's salts, 2.0 mM L-glutamine, 10% FBS, 10 IU mL⁻¹ penicillin (Gibco), 10 µg mL⁻¹ streptomycin (Gibco), and 0.05 IU mL⁻¹ porcine FSH (FSH+; Sigma Aldrich) or vehicle control (CTL). Both IVM media were adjusted for pH (7.2–7.4) and osmolarity (260–280 mOsm). The COCs were randomly divided in groups of 20–25 in 150 µL of IVM media (Van Tol et al., 1996) and incubated with 5% CO₂, saturated humidity, at 38.5 °C for 22 h.

COCs were denuded after IVM in 0.2% hyaluronidase (Sigma Aldrich) with gentle pipetting. Pools of CCs were obtained from 80 to 150 COCs and washed in 1.0 mL PBS without calcium and magnesium (PBS^{-Ca-Mg}; Sigma Aldrich), and centrifuged at 2,000 g for five minutes. The cell pellet was resuspended in 100 µL PBS^{-Ca-Mg}, snap frozen in liquid nitrogen, and stored at – 80 °C.

Total RNA extraction and cDNA synthesis

The total RNA extraction was carried out with the ReliaPrep RNA Cell Miniprep kit (Promega). The total RNA was initially quantified and evaluated using Nanodrop 2000 C (Thermo Scientific) to determine 260/280 and 260/230 ratios. The total RNA integrity was evaluated by electrophoresis in 1.0% agarose gels, and samples were stained with Blue Green Loading Dye (LGC Biotecnologia). The electrophoresis was carried out in 0.5X TBE buffer at 80 V, 120 A for 40 min. Finally, the total RNA was also quantified by Qubit (Invitrogen) to carry out the reverse transcription (RT) reaction (cDNA synthesis).

The cDNA synthesis was performed immediately after total RNA extraction and quantifications. The procedure was carried out with QuantiTect RT Kit (Qiagen). Putative residual DNA was removed from samples by the genomic DNA elimination reaction (500 ng total RNA and 2.0 µL 7X wipeout buffer in a 14 µL solution) incubated at 42 °C for 3 min and transferred to 4 °C immediately. The wipeout reaction was mixed to the RT reaction (4.0 µL 5X RT Buffer, 1.0 µL Quantiscript RT, and 1.0 µL Primer mix) and incubated at 42 °C for 30 min. Additionally, samples were incubated at 95 °C for 3 min for RT inactivation and stored at – 20 °C.

Reverse transcription quantitative PCR (RT-qPCR)

Most primers were from a multi-species primer set (Table 1). Alternatively, primers were designed as described by Moura



Table 1. Primers used for reverse transcription quantitative PCR (RT-qPCR)

Gene symbols	Primers (F: Forward/R: Reverse)	Amplicon (bp)	Accession number (Species)	Ref.
<i>B-ACTIN</i>	F: TGGCACCACACCTTCTACAAC R: GGTCATCTTCTCACGGTTGG	105	JX046106.1 (<i>Capra hircus</i>)	1
<i>ATP1A1</i>	F: GCAGGGGATGAAGAACAAGA R: GAGAAGCGAGTAGGGGAAGG	154	NM_001009360.1 (<i>Ovis aries</i>)	2
<i>GAPDH</i>	F: TGGAGGGACTTATGACCACTG R: AGAAGCAGGGATGATGTTCTG	119	gi27525390 (<i>Capra hircus</i>)	3
<i>H3F3A</i>	F: ACTGGAGGGGTGAAGAAACC R: CCTCACTTGCCTCCTGCAAA	199	NM_001014389.2 (<i>Bos taurus</i>)	2
<i>PPIA</i>	F: GACTGAGTGGTTGGATGGCA R: GCCATTTCTGGACCCAAAGC	97	NM_001308578.1 (<i>Ovis aries</i>)	2
<i>RPL19</i>	F: ATGAAATCGCCAATGCCAAC R: GGCAGTACCCTTTCGCTTACC	167	gi94966830 (<i>Bos taurus</i>)	1
<i>SDHA</i>	F: GGAGCTGGAGAATTACGGCA R: CGCAGGGACCTTCCATACAA	177	XM_012125144.1 (<i>Ovis aries</i>)	3
<i>TBP</i>	F: AGAATAAGAGAGCCCCGCAC R: TTCTTCACTCTTGGCTCCCC	78	XM_012166509.1 (<i>Ovis aries</i>)	3
<i>UBB</i>	F: GCATTGTTGGGTTCTGTGTC R: CACGAAGATTTGCATTTTGAC	98	NM_001009202.1 (<i>Ovis aries</i>)	2
<i>YWHAZ</i>	F: CCGGACACAGAACATCCAGTC R: CTCCAAGATGACCTACGGGC	200	NM_174814.2 (<i>Bos taurus</i>)	2
<i>HAS2</i>	F: GCCGGTCTGCTCAAATTCATC R: ACAATGCATCTTGTTCAGCTC	129	NM_174079.2 (<i>Bos taurus</i>)	This study
<i>MYC</i>	F: ACTCCACCGCCTTTTCTCC R: CTTGTTCTTCTCAGAGTCGC	135	NM_001046074.2 (<i>Ovis aries</i>)	3
<i>PTGS2</i>	F: GGAAAGAACCATGGGGTGGGA R: CCATCCTTGAAAAGGCGCAG	83	XM_012186886.1 (<i>Ovis aries</i>)	This study
<i>THAP11</i>	F: CACGGGAGAAGACGTTAAGC R: GGAGCCAGTATCAGGGAAGC	187	NM_001104994 (<i>Bos taurus</i>)	1
<i>ZFX</i>	F: TCCTTGGATGATGCTGGCAA R: CAGTCCCACCTAAGTCATATC	163	NM_177490.1 (<i>Bos taurus</i>)	3
<i>ZNF281</i>	F: TCCAAATACCTCCAACAGGC R: GGCAATGAAGATGGCAACAC	194	XM_610917.6 (<i>Bos taurus</i>)	1

1: Moura et al. (2018). 2: Moura et al. (2019). 3: Silva et al. (2018). Bp: base pair. B-ACT: β -Actin. ATP1A1: ATPase Na⁺/K⁺ Transporting Subunit Alpha 1. GAPDH: Glyceraldehyde 3-phosphate Dehydrogenase. H3F3A: H3 histone, family 3A. PPIA: Peptidylprolyl Isomerase A. RPL19: Ribosomal Protein L19. SDHA: Succinate Dehydrogenase Complex Flavoprotein Subunit A. TBP: TATA-Box Binding Protein. UBB: Ubiquitin B. YWHAZ: Tyrosine 3-Monooxygenase/Tryptophan 5-Monooxygenase activation Protein Zeta. MYC Proto-Oncogene, BHLH Transcription Factor. PTGS2: Prostaglandin-Endoperoxide Synthase 2. THAP11: THAP Domain Containing 11. ZFX: Zinc Finger Protein X-Linked. ZNF281: Zinc Finger Protein 281.

et al. (2018). The nucleotide sequences of gene transcripts of three species (i.e., *Capra hircus*, *Ovis aries*, and *Bos taurus*) were retrieved from GenBank (<https://www.ncbi.nlm.nih.gov/genbank/>). Primers were designed using Primer-BLAST (<https://www.ncbi.nlm.nih.gov/tools/primer-blast/>) and further screened using Primer3plus (<https://www.bioinformatics.nl/cgi-bin/primer3plus/primer3plus.cgi>). The primers' design aimed for amplicons with 70–200 base pairs (bp), length of 19–23 nucleotides, 40–60% GC content, and low predictions of primer-dimer formation. Selected primers (Table 1) were predicted as specific and eligible as multi-species qPCR primers.

RT-qPCR was carried out using the SYBR Green detection system (LineGene 9660, model FQD-96A – Bioer). The reaction was carried out with 1.0 μ L cDNA, 5.0 μ L 2X Go Taq qPCR Master Mix (Promega), 3.4 μ L ultra-pure H₂O and 0.6 μ L primers (2.5 μ M) in a final volume of 10 μ L. The cDNA was used as diluted samples (1:10) after primer efficiency testing (described below). The RT-qPCR reactions

were carried out as follows: initial denaturation at 95 °C for 2 min, followed by 40 cycles at 95 °C for 15 s (denaturation), and 60 °C for 60 s (both annealing and extension). The melting curves were analysed from 65 to 95 °C for 20 min after the qPCR cycles. Relative gene expression levels were based on the number of cycles to reach the detection threshold (i.e., quantification cycle – Cq) during the exponential phase of the qPCR reaction.

Primer efficiency was calculated by a five-point standard curve methodology using cDNA serial dilution: 1⁰ (non-diluted), 10⁻¹, 10⁻², 10⁻³, and 10⁻⁴ as carried out by Silva et al. (2014). Each primer efficiency was determined using the amplification curve ($E = 10^{-1/\text{slope}}$), Pearson's correlation coefficient (R), and interception (y).

Relative gene expression analysis was carried out using three biological replicates, three technical replicates (for each biological replicate), and three RGs. The relative gene expression was determined by the 2^{- $\Delta\Delta$ Ct} method using the



Relative Expression Software Toll (REST) software (Livak and Schmittgen, 2001) by paired comparisons using randomisation and bootstrapping (Pfaffl et al., 2002).

Selection of reference genes

Candidate RGs were tested for stability values using GeNorm (Vandesompele et al., 2002), BestKeeper (Pfaffl et al., 2004), NormFinder (Andersen et al., 2004), the comparative Delta CT method (Silver et al., 2006), and RefFinder (Xie et al., 2012). The GeNorm software calculates an RG stability value (M -value) and establishes an RG index. The mean M -value is a parameter for selecting the most appropriate RGs (Vandesompele et al., 2002). BestKeeper (version 1) computes stability values based on raw Cq values, while potential RGs must hold standard deviation (SD) values of <1.0 . The correlation coefficient of BestKeeper selects the most stable RGs and calculates the potential of multiple RGs at once (Pfaffl et al., 2004). The NormFinder software was also carried out to rank the most stable RGs (and best RG pair) assuming both intra-group and inter-group variation with mixed linear effects (Andersen et al., 2004). The comparative delta CT method performs delta Cq comparisons between RGs pairs (Silver et al., 2006). The RefFinder software (www.heartcure.com.au/reffinder/?type=reference) makes a unified ranking of RGs based on GeNorm, NormFinder, BestKeeper, and the Delta CT method (Xie et al., 2012).

In silico predictions of gene regulation and signalling networks

The genomic contexts of *MYC* and *THAP11* loci were retrieved from NCBI (www.ncbi.nlm.nih.gov/gene/). DNA sequences of *MYC* and *THAP11* gene bodies [transcription start site (TSS) to the end of the transcript] and promoter regions (2.5 kb sequence upstream of the TSS) were retrieved from GenBank in May 2020 (File S1). Transcription factor binding sites (TFBS) were predicted in *MYC* and *THAP11* loci (gene bodies and promoters) using PROMO 3.0 (Farré et al., 2003) and TRANSFAC database version 8.3 (algen.lsi.upc.es/recerca/menu_recerca.html). The prediction of TFBS was done for twelve selected TFs from the literature (Table S1).

Both *MYC* and *THAP11* reference proteins were retrieved from GenBank in May 2020 (<https://www.ncbi.nlm.nih.gov/protein/>).

Potential phosphorylation sites associated with signal transduction of EGFR, ERK, GS3K β , JAK/STAT, P38, PI3K/AKT, and PKA signalling pathways were predicted using both NetPhos 3.1 (www.cbs.dtu.dk/services/NetPhos/) and Scansite 4.0 (scansite4.mit.edu/4.0/#home) using the default options. The sequence of DNA-binding and transactivation domains were obtained from the literature and annotated manually.

The protein–protein interaction (PPI) network was predicted with STRING version 11.5 using the multiple proteins default search for *Bos taurus* (<https://string-db.org/>). The proteins used for the PPI network included core components of FSH and EGFR signalling networks (Table S2). Network clustering was based on ‘k-means clustering’ for three clusters.

RESULTS

Experimental design and RT-qPCR primer efficiency

The experimental design envisioned testing if candidate TFs (Table S1) have their gene expression levels affected by FSH availability (Fig. 1). Hallmarks of FSH-mediated effects were absent under CTL conditions (e.g., lower nuclear maturation efficiency, diminished expansion of CCs), which were described elsewhere (Cantanhêde et al., 2021). Therefore, these results validated the experimental design at the cellular level in this previous study.

RGs must be selected under strict conditions to ensure accurate RT-qPCR conditions. From ten candidate RGs (Table 1), seven showed melting curves which suggest single amplicons (data not shown). Based on the five-point standard curve, RGs showed adequate efficiencies (97.20–105.96%), with correlation coefficients ranging from -0.985 to -0.999 , and slopes varying from -3.19 to -3.39 (Table 2). These seven candidates underwent a further selection of the most stable RGs.

Selection of reference genes

The GeNorm software showed UBB and YWHAZ as the best pair of RGs ($M = 0.604$), while ATP1A1 ($M = 0.724$) was the third most stable RG (Fig. 2A). BestKeeper found GAPDH (SD = 0.488), ATP1A1 (SD = 0.873) and YWHAZ (SD = 0.907) as the three most stable RGs (Fig. 2B). The

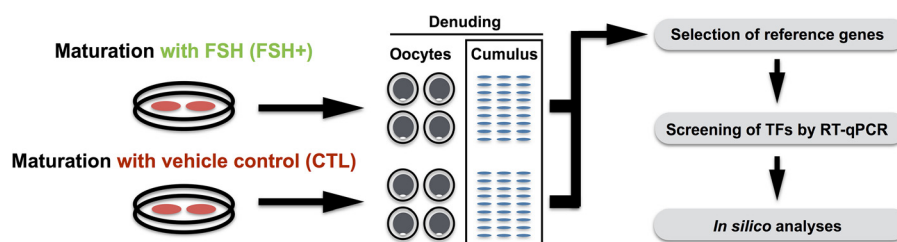


Fig. 1. Experimental design. Retrieval of cumulus-oocyte complexes (COCs) and *in vitro* maturation (IVM) under FSH-containing (FSH+) and vehicle-containing (control, CTL) media for 22 h. Collection of cumulus cells (CCs) occurred after oocyte denuding and CCs underwent gene expression analysis of candidate transcription factors (TFs) by reverse transcription quantitative PCR (RT-qPCR). *In silico* analyses relied on *in silico* tools for TF binding sites, post-translation modifications (phosphorylation sites), and protein–protein interaction networks

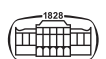


Table 2. Primer parameters and efficiency analysis derived from RT-qPCR reactions

Gene symbol	T _m (°C)	Mean (C _q)	Primer efficiency %	NTC (C _q)	Pearson's correlation coefficient (R)	Slope	Y Intercept
<i>B-ACTIN</i>	84.83	17.12	103.78	30.02	-0.999	-3.23	26.91
<i>ATP1A1</i>	81.69	18.31	101.08	ND	-0.989	-3.30	26.09
<i>GAPDH</i>	85.43	16.16	100.60	ND	-0.985	-3.31	24.06
<i>H3F3A</i>	82.68	16.67	105.96	ND	-0.996	-3.19	25.31
<i>PPIA</i>	81.15	16.77	103.12	30.79	-0.997	-3.25	27.42
<i>UBB</i>	80.98	18.46	102.84	34.79	-0.995	-3.26	26.81
<i>YWHAZ</i>	82.09	18.74	97.20	ND	-0.985	-3.39	27.61
<i>HAS2</i>	81.11	19.74	98.43	ND	-0.989	-3.36	31.69
<i>MYC</i>	85.75	21.23	97.44	ND	-0.970	-3.38	32.47
<i>PTGS2</i>	76.42	22.64	94.70	ND	-0.927	-3.46	32.47
<i>THAP11</i>	89.63	22.28	102.65	ND	-0.959	-3.26	35.46
<i>ZFX</i>	80.23	21.41	102.48	ND	-0.991	-3.26	32.58
<i>ZNF281</i>	80.78	20.80	95.21	ND	-0.997	-3.44	32.13

C_q: quantification cycle. ND: Not detected. NTC: no template control. T_m: melting temperature. B-ACT: β -Actin. ATP1A1: ATPase Na⁺/K⁺ Transporting Subunit Alpha 1. GAPDH: Glyceraldehyde 3-phosphate Dehydrogenase. H3F3A: H3 histone, family 3A. PPIA: Peptidylprolyl Isomerase A. UBB: Ubiquitin B. YWHAZ: Tyrosine 3-Monooxygenase/Tryptophan 5-Monooxygenase activation Protein Zeta. HAS2: Hyaluronan Synthase 2. MYC Proto-Oncogene, BHLH Transcription Factor. PTGS2: Prostaglandin-Endoperoxide Synthase 2. THAP11: THAP Domain Containing 11. ZFX: Zinc Finger Protein X-Linked. ZNF281: Zinc Finger Protein 281.

most stable RG by NormFinder was ATP1A1 ($M = 0.346$), while YWHAZ ($M = 0.357$) and UBB ($M = 0.535$) were the second and third most stable RGs, respectively (Fig. 2C). The comparative Delta-CT method revealed YWHAZ and ATP1A1 as the best RGs, while UBB was the third most stable RG (Fig. 2D). A comprehensive ranking by RefFinder revealed YWHAZ, ATP1A1, and UBB as the most stable RGs (Fig. 3). Nonetheless, the GeNorm pairwise analysis

indicated that six RGs were the closest scenario to the software cut-off value (Fig. 3).

Gene expression analysis

The investigation of FSH-responsive genes by RT-qPCR aimed to validate the experimental model at the molecular level. Primer specificity and efficiency supported the screening

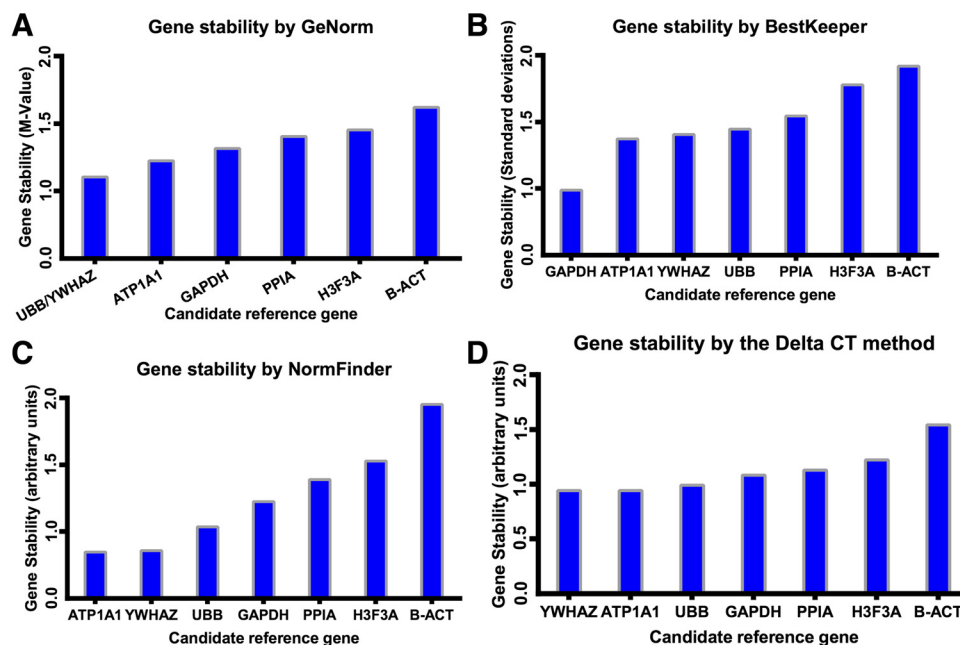


Fig. 2. Gene expression stability values for seven candidate reference genes (RGs) in cumulus cells treated with FSH (FSH+) or the vehicle control (CTL) during *in vitro* maturation of bovine cumulus-oocyte complexes. A) GeNorm software. The ranking begins with the best pair of RGs (lowest M-values combined) on the far right followed by RGs with increasing M-values (from right to left). B) Bestkeeper software. C) Normfinder software. D) The comparative Delta CT method. B-ACT: β -Actin. ATP1A1: ATPase Na⁺/K⁺ Transporting Subunit Alpha 1. GAPDH: Glyceraldehyde 3-phosphate Dehydrogenase. H3F3A: H3 histone, family 3A. PPIA: Peptidylprolyl Isomerase A. UBB: Ubiquitin B. YWHAZ: Tyrosine 3-Monooxygenase/Tryptophan 5-Monooxygenase activation Protein Zeta



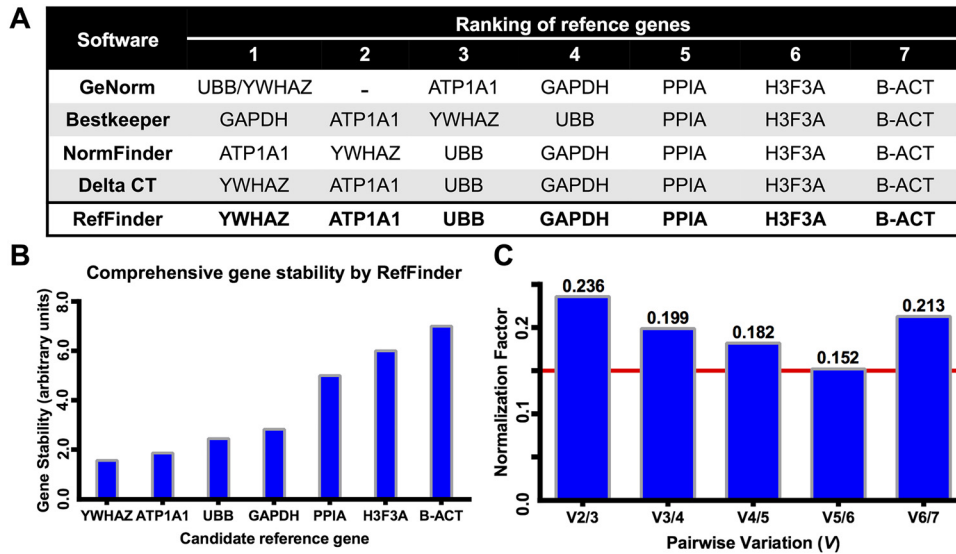


Fig. 3. Comprehensive ranking of reference genes (RGs) and their index prediction. A) Summary of RGs rankings by five software. B) Comprehensive ranking and overall gene stability values by RefFinder. C) GeNorm pairwise analysis for index prediction of RGs. B-ACT: β -Actin. ATP1A1: ATPase Na⁺/K⁺ Transporting Subunit Alpha 1. GAPDH: Glyceraldehyde 3-phosphate Dehydrogenase. H3F3A: H3 histone, family 3A. PPIA: Peptidylprolyl Isomerase A. UBB: Ubiquitin B. YWHAZ: Tyrosine 3-Monooxygenase/Tryptophan 5-Monooxygenase Activation Protein Zeta

candidate TFs (Table 2). HAS2 relative expression was higher in FSH+ (2.39-fold; $P = 0.003$), albeit PTGS2 gene transcript levels were similar between FSH+ and CTL ($P = 0.37$; Fig. 4). Among candidate TFs, the expression level of both ZFX ($P = 0.45$) and ZNF281 ($P = 0.296$) did not differ between groups (Fig. 4). The relative expression of MYC was lower in FSH+ by 0.35-fold ($P < 0.0001$), while THAP11 was higher by 1.47-fold ($P = 0.016$; Fig. 4).

Integrating MYC and THAP11 into FSH signalling networks

To explore the potential connection between FSH signalling with MYC and THAP11 gene expression, *in silico* analyses predicted regulatory modes at transcriptional and post-transcriptional levels (Fig. 5). The genomic context highlighted the location of MYC and THAP11, their neighbouring genes, and the DNA strand where transcription occurs (Fig. 5A).

TFBS mapping for twelve FSH-responsive TFs (Table S1) found multiple sites within MYC and THAP11 gene bodies and promoters (Fig. 5B; Table S3). The exception to this rule was P53, with no predicted TFBS at MYC and THAP11 gene bodies and promoters. MYC displayed TFBS at the exon six of MYC and the THAP11 promoter (Fig. 5B), thus suggesting potential direct cross-talk. The prediction of phosphorylation sites showed sites for GS3K, PKA, and P38 signalling (Fig. 5C). Nonetheless, EGFR-mediated phosphorylation was only on the MYC protein (Fig. 5C).

The PPI analysis showed a network of highly clustered connections, with three subnetworks (Fig. 5D). MYC is part of the main subnetwork with most nodes and edges. Further, MYC has edges with several components of GS3K signalling,

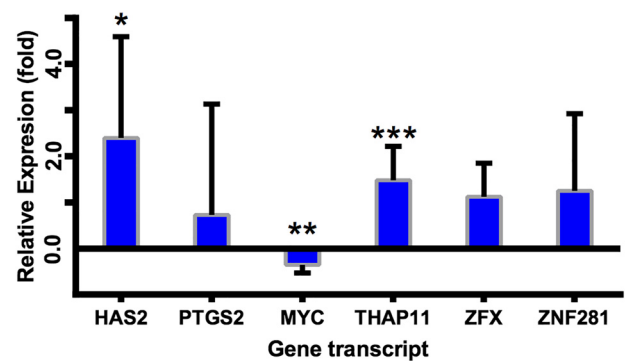
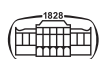


Fig. 4. Relative expression of six candidate gene transcripts in cumulus cells treated with FSH (FSH+) or the vehicle control (CTL) during *in vitro* maturation of bovine cumulus-oocyte complexes. Relative expression (arbitrary units of fold change): FSH+ compared to the CTL threshold. Error bar: standard error of the mean. HAS2: Hyaluronan Synthase 2. PTGS2: Prostaglandin-Endoperoxide Synthase 2. MYC: MYC Proto-Oncogene, BHLH Transcription Factor. THAP11: THAP Domain Containing 11. ZFX: Zinc Finger Protein X-Linked. ZNF281: Zinc Finger Protein 281. * $P = 0.003$. ** $P < 0.0001$. *** $P = 0.016$

alongside edges with EGFR, ERK, JAK/STAT, and PI3K pathways (Fig. 5D). MYC also forms edges with several FSH-responsive TFs. MYC connects indirectly to the FSHR subnetwork via FOXO1 (Fig. 5D). There is no link between THAP11 and the FSH signalling network whatsoever, so it forms an independent subnetwork (Fig. 5D). The integration of experimental and *in silico* analyses culminate in a roadmap to dissect the potential contribution of MYC to FSH signalling in CCs during the acquisition of oocyte competence (Fig. 6).



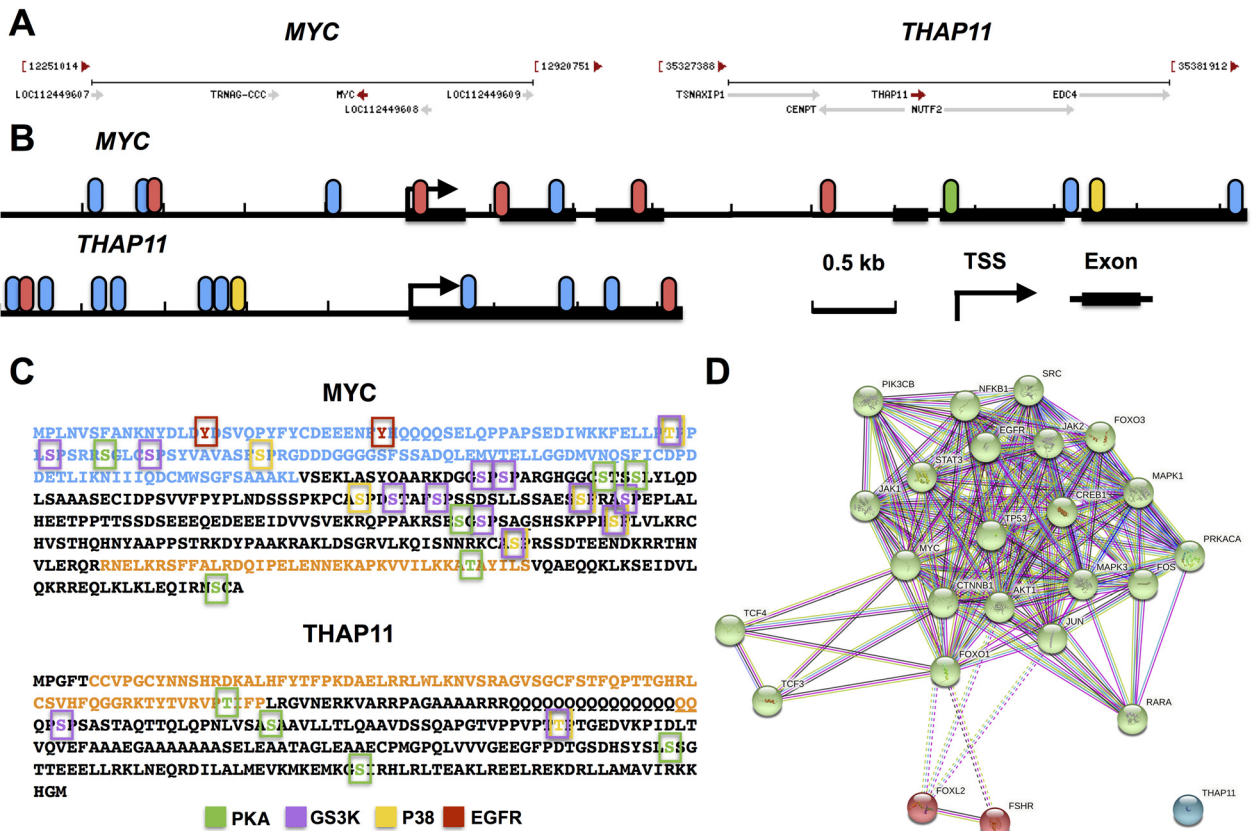


Fig. 5. *In silico* predictions of *MYC* and *THAP11* transcriptional and post-translational regulation by FSH signalling networks. A) Genomic context of *MYC* and *THAP11* genes in the *Bos taurus* genome (www.ncbi.nlm.nih.gov/gene/). Red arrows determine the direction of transcription. B) Schematic representation of selected transcription factor binding sites (TFBS) at *MYC* and *THAP11* promoters (2.5 kb upstream sequences) and gene bodies using PROMO 3.0. TFBS representation: CREB (green), FOXO1 (blue), MYC (yellow), and TCF4 (red). Arrows indicate transcription start sites (TSS) and black rectangles represent exons. C) Phosphorylation sites in *MYC* and *THAP11* proteins predicted by NetPhos 3.1 and Scansite 4.0. Potential phosphorylation sites predicted (coloured squares) as downstream signals of Epidermal Growth Factor Receptor (EGFR), Glycogen Synthase Kinase 3 (GSK3), p38 MAPK (Mitogen-Activated Protein Kinase), Protein Kinase A (PKA) pathways. Transactivation domain highlighted in blue fonts and DNA-binding domains in orange fonts. D) Protein-protein interaction network predicted with STRING software v11.5 (see material and methods). Nodes described as coloured circles. Differences in node colours represent different subnetworks revealed by K-mean clustering. Lines (edges) between nodes describe connections (interactions) between proteins. Known interactions: light blue edges (from curated databases) and pink edges (experimentally determined). Predicted interactions: green edges (gene neighbourhood), and dark blue edges (gene co-occurrence). Other: yellow edges (text mining) and black edges (co-expression)

DISCUSSION

A comprehensive screening found *ATP1A1*, *UBB*, and *YWHAZ* as the three most stable RGs in CCs under varying FSH conditions. Primers of candidate RGs were specific and had adequate amplification efficiencies, thus ruling out potential technical limitations on the RGs screening. The five software mostly converged on these three RGs as the most stable across samples. Since RGs found here did not reach the GeNorm pairwise cutoff (Vandesompele et al., 2002), it suggests that further screenings with other candidate RGs could lead to more reliable RT-qPCR normalisation. Other similar studies found different RGs (O'Connor et al., 2013; Khan et al., 2015; Wang et al., 2017), possibly due to different candidate RGs but also likely due to experimental and technical factors. Collectively, these reports reinforce the

need to validate RGs for each experiment to counterbalance bias from technical and biological factors (O'Connor et al., 2013; Wang et al., 2017; Taylor et al., 2019).

The gene transcript levels of FSH-responsive gene *HAS2* was higher while *PTGS2* was similar to CTL in CCs under FSH-containing conditions, respectively. These results validated the experimental design. *HAS2* is an enzyme responsible for hyaluronic acid synthesis, which mediates the expansion of CCs during oocyte maturation (Schoenfelder and Einspanier, 2003; Assidi et al., 2008). The hyaluronic acid maintains CCs attached to the oocyte but with less adhesion among them, thus facilitating the passage of sperm cells during fertilisation (Schoenfelder and Einspanier, 2003; Assidi et al., 2008). The induction of *HAS2* transcription by FSH was previously described (Schoenfelder and Einspanier, 2003; Richards, 2005). FSH did not affect



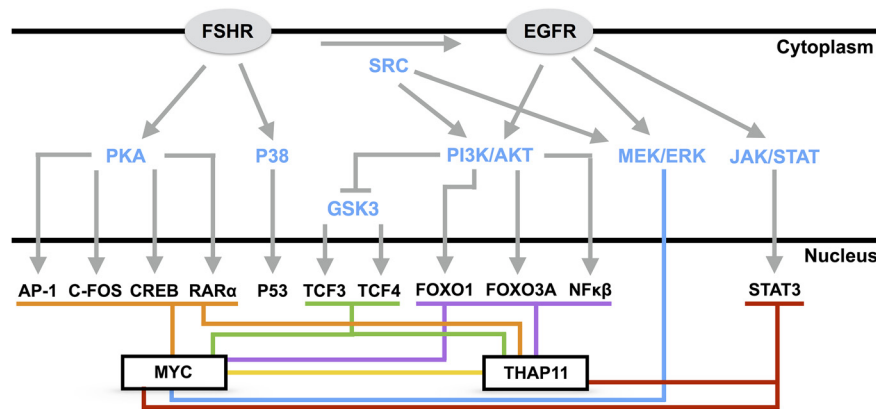


Fig. 6. MYC and THAP11 in the FSH signalling networks. FSHR and EGF signalling activates PKA, P38, PI3K/AKT, MEK/ERK, and JAK/STAT pathways (highlighted as blue fonts). FSHR and EGFR signalling pathways are connected by the SRC pathway. Several transcription factors (TFs) have predicted transcription factor binding sites (TFBS) in the promoter (*i.e.*, 2.5 kb upstream sequences) and/or gene bodies of MYC and THAP11 *Bos taurus* orthologues (described as coloured lines connecting TFs). TFBS were predicted using PROMO 3.0 software (see Material and methods). The connection between ERK and MYC occurs directly by phosphorylation, which leads to MYC down-regulation (Wang et al., 2006)

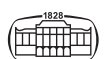
PTGS2 (also known as cyclooxygenase enzyme 2 – COX2) levels in CCs after oocyte maturation. PTGS2 is an enzyme that participates in the conversion of arachidonic acid into prostaglandins (Assidi et al., 2008; Marei et al., 2014), which are active mediators of several reproductive processes, such as the expansion of CCs and ovulation (Assidi et al., 2008; Marei et al., 2014). Gonadotropins induce the transcription of PTGS2 in CCs within a few hours of exposure (Nuttinck et al., 2002, 2004; Marei et al., 2014), although it returns to basal gene transcript levels at the end of IVM (Marei et al., 2014), as described here.

The exposure of CCs to FSH culminated at lower MYC and higher THAP11 gene transcript levels. These two protein-coding genes are master regulators of cellular state by modulating metabolic and other core cellular processes (Eilers and Eisenman, 2008; Dejosez et al., 2010; Rahl and Young, 2014; Fujita et al., 2017). CCs transcribe both MYC and THAP11 (Miles et al., 2012; Mao et al., 2014; Moura et al., 2018). The inhibition of FSHR diminished MYC mRNA and protein levels in sheep COCs and ovarian cancer cells (Wei et al., 2018; Yang et al., 2019). The differentiation of bovine granulosa cells by lactate (which mimics a pre-ovulatory cellular phenotype) led to MYC down-regulation (Baufeld et al., 2019). The discrepancy between MYC up-regulation or down-regulation under FSH exposure is likely due to the biphasic nature of early responsive genes, with rapid response and later repression, as described above for *PTGS2*. Hence, there is no evidence of the connection of THAP11 to FSH signalling networks.

Predictions revealed numerous potential TFBS in both MYC and THAP11 cis-regulatory elements. Two facts highlight the importance of these findings. Cell identity and cellular processes involve the engagement of multiple TFs for modulating specific gene sets (Olson, 2006; Vinayagam et al., 2011). Further, the predictions covered DNA sequences (–300/+100 bp from the TSS) which contain most TFBS in bovine genes (Goszczyński et al., 2021). Additional

evidence of a connection between these TFs with FSH signalling came from predictions of protein post-translational modifications. *In silico* analyses also found potential phosphorylation sites in both MYC and THAP11 proteins, which suggest downstream cues of both FSHR and EGFR signalling pathways. These predictions include previously characterised phosphorylation sites (threonine 58 and serine 62 in MYC), which stem from mitogenic signals and lead to protein degradation (Sears et al., 2000). The PPI network revealed another layer of evidence of MYC connection to FSH signalling. MYC has several edges in the network with factors from multiple FSH downstream pathways. The network also predicts that MYC integrates GSK3 signalling into the core FSH/EGFR subnetwork. THAP11 has no interactions with core components of the PPI network and may play independent roles in cellular identity and function of CCs, as demonstrated in embryonic stem cells (Dejosez et al., 2008, 2010). Since the PPI network combines multiple datasets (Szklarczyk et al., 2021), it represents more solid evidence that THAP11 is not part of the FSH signalling network. Under this scenario, the higher gene transcript levels of THAP11 under FSH may be an indirect event during oocyte maturation.

The combination of experimental and *in silico* evidence is promising to unravel details of FSH signalling. Nonetheless, more experimental exploration will settle details of potential connections between TFs and signalling pathways, such as expanding gene interactions and detailing network motifs. For instance, THAP11 represses MYC in both mouse and human cancer cells (Nakamura et al., 2012; Zhang et al., 2020). The genome-wide mapping of MYC binding sites should unravel the identity of its target genes during oocyte maturation, while THAP11 mapping will contribute to an understanding of FSH-independent processes during oocyte maturation. Further genome-wide TFBS mapping will reveal network motifs, such as negative and positive auto-regulatory loops. Therefore, MYC integrates the FSH signalling



network in CCs and may contribute to understanding the pleiotropic effects of this gonadotropin during the acquisition of oocyte competence.

ACKNOWLEDGEMENTS

We would like to thank all laboratory members for their contributions and insightful discussions. Authors would like to acknowledge CNPq for the doctorate degree scholarship (LFC). This project was supported by CAPES post-doctorate fellowship (MTM; Financial code 001). Additionally, authors would like to acknowledge FACEPE (grant APQ-1101-5.05-15), CNPq and CAPES (Rede Intersys: Biologia sistêmica no estudo de função gênica em interações bióticas, Edital CAPES 51/2013) for the financial support of the study.

SUPPLEMENTARY MATERIAL

Supplementary data to this article can be found online at <https://doi.org/10.1556/004.2022.00007>.

REFERENCES

- Andersen, C. L., Jensen, J. L. and Ørntoft, T. F. (2004): Normalization of real-time quantitative reverse transcription-PCR data: a model-based variance estimation approach to identify genes suited for normalization, applied to bladder and colon cancer data sets. *Cancer Res.* **64**, 5245–5250.
- Andrade, G. M., Del Collado, M., Meirelles, F. V., Da Silveira, J. C. and Perecin, F. (2019): Intrafollicular barriers and cellular interactions during ovarian follicle development. *Animal Reprod.* **16**, 485–496.
- Assidi, M., Dufort, I., Ali, A., Hamel, M., Algriany, O., Dielemann, S. and Sirard, M. A. (2008): Identification of potential markers of oocyte competence expressed in bovine cumulus cells matured with follicle-stimulating hormone and/or phorbol-myristate acetate *in vitro*. *Biol. Reprod.* **79**, 209–222.
- Assidi, M., Richard, F. J. and Sirard, M. A. (2013): FSH *in vitro* versus LH *in vivo*: similar genomic effects on the cumulus. *J. Ovarian Res.* **6**, 68.
- Baufeld, A., Koczan, D. and Vanselow, J. (2019): L-lactate induces specific genome wide alterations of gene expression in cultured bovine granulosa cells. *BMC Genom.* **20**, 273.
- Blaha, M., Nemcova, L., Kepkova, K. V., Vodicka, P. and Prochazka, R. (2015): Gene expression analysis of pig cumulus-oocyte complexes stimulated *in vitro* with follicle stimulating hormone or epidermal growth factor-like peptides. *Reprod. Biol. Endocrinol.* **6**, 113.
- Cantanhêde, L. F., Santos-Silva, C. T., Moura, M. T., Gonçalves, D. N., Ferreira-Silva, J. C., Oliveira, J. M., Teixeira, A. A., Wanderley-Teixeira, V. and Oliveira, M. A. L. (2021): FSH mediates the consumption of serum-derived glycogen by bovine cumulus-oocyte complexes during *in vitro* maturation. *Vet. World* **14**, 2512–2517.
- Casarini, L. and Crépieux, P. (2019): Molecular mechanisms of action of FSH. *Frontiers Endocrinol.* **10**, 305.
- Chapman, J. R. and Waldenström, J. (2015): With reference to reference genes: a systematic review of endogenous controls in gene expression studies. *PLoS One* **10**, e0141853.
- Dejosez, M., Krumenacker, J. S., Zitur, L. J., Passeri, M., Chu, L.-F., Songyang, Z., Thomson, J. A. and Zwaka, T. P. (2008): Ronin is essential for embryogenesis and the pluripotency of mouse embryonic stem cells. *Cell* **27**, 1162–1174.
- Dejosez, M., Levine, S. S., Frampton, G. M., Whyte, W. A., Stratton, S. A., Barton, M. C., Gunaratne, P. H., Young, R. A. and Zwaka, T. P. (2010): Ronin/Hcf-1 binds to a hyperconserved enhancer element and regulates genes involved in the growth of embryonic stem cells. *Genes Dev.* **24**, 1479–1484.
- Eilers, M. and Eisenman, R. N. (2008): Myc's broad reach. *Genes Dev.* **15**, 2755–2766.
- Farré, D., Roset, R., Huerta, M., Adsuara, J. E., Roselló, L., Albà, M. M. and Messeguer, X. (2003): Identification of patterns in biological sequences at the ALGGEN server: PROMO and MALGEN. *Nucleic Acids Res.* **31**, 3651–3653.
- Fujita, J., Freire, P., Coarfa, C., Benham, A. L., Gunaratne, P., Schneider, M. D., Dejosez, M. and Zwaka, T. P. (2017): Ronin governs early heart development by controlling core gene expression programs. *Cell Rep.* **21**, 1562–1573.
- Gloaguen, P., Crépieux, P., Heitzler, D., Poupon, A. and Reiter, E. (2011): Mapping the follicle-stimulating hormone-induced signaling networks. *Front. Endocrinol.* **2**, 45.
- Goszczynski, D. E., Halstead, M. M., Islas-Trejo, A. D., Zhou, H. and Ross, P. J. (2021): Transcription initiation mapping in 31 bovine tissues reveals complex promoter activity, pervasive transcription, and tissue-specific promoter usage. *Genome Res.* **31**, 732–744.
- Herndon, M. K., Law, N. C., Donaubaauer, E. M., Kyriss, B. and Hunzicker-Dunn, M. (2016): Forkhead box O member FOXO1 regulates the majority of follicle-stimulating hormone responsive genes in ovarian granulosa cells. *Mol. Cell. Endocrinol.* **434**, 116–126.
- Khan, D. R., Guillemette, C., Sirard, M. A. and Richard, F. J. (2015): Characterization of FSH signalling networks in bovine cumulus cells: a perspective on oocyte competence acquisition. *Mol. Hum. Reprod.* **21**, 688–701.
- Kuo, F. T., Fan, K., Bentsi-Barnes, I., Barlow, G. M. and Pisarska, M. D. (2012): Mouse forkhead L2 maintains repression of FSH-dependent genes in the granulosa cell. *Reproduction* **144**, 485–494.
- Livak, K. J. and Schmittgen, T. D. (2001): Analysis of relative gene expression data using real-time quantitative PCR and the $2^{-\Delta\Delta CT}$ method. *Methods* **25**, 402–408.
- Lonergan, P. and Fair, T. (2016): Maturation of oocytes *in vitro*. *Ann. Rev. Anim. Biosci.* **4**, 255–268.
- Macaulay, A. D., Gilbert, I., Scantland, S., Fournier, E., Ashkar, F., Bastien, A., Saadi, H. A., Gagne, D., Sirard, M. A., Khandjian, E. W., Richard, F. J., Hyttel, P. and Robert, C. (2016): Cumulus cell transcripts transit to the bovine oocyte in preparation for maturation. *Biol. Reprod.* **94**, 16.
- Mao, J., Zhang, Q., Ye, X. Y., Liu, K. and Liu, L. (2014): Efficient induction of pluripotent stem cells from granulosa cells by Oct4 and Sox2. *Stem Cells Dev.* **23**, 779–789.



- Marei, W. F., Abayasekara, D. R. E., Wathes, D. C. and Fouladi-Nashta, A. A. (2014): Role of PTGS2-generated PGE2 during gonadotrophin-induced bovine oocyte maturation and cumulus cell expansion. *Reprod. Biomed. Online* **28**, 388–400.
- Miles, J. R., McDaneld, T. G., Wiedmann, R. T., Cushman, R. A., Echternkamp, S. E., Vallet, J. L. and Smith, T. P. L. (2012): MicroRNA expression profile in bovine cumulus-oocyte complexes: possible role of let-7 and miR-106a in the development of bovine oocytes. *Anim. Reprod. Sci.* **130**, 16–26.
- Moura, M. T., Silva, R. L. O., Cantanhêde, L. F., Silva, J. B., Ferreira-Silva, J. C., Silva, P. G., Ramos-Deus, P., Pandolfi, V., Kido, E. A., Benko-Iseppon, A. M. and Oliveira, M. A. (2018): Activity of non-canonical pluripotency-associated transcription factors in goat cumulus-oocyte complexes. *Livestock Sci.* **212**, 52–56.
- Moura, M. T., Silva, R. L., Nascimento, P. S., Ferreira-Silva, J. C., Cantanhêde, L. F., Kido, E. A., Benko-Iseppon, A.M. and Oliveira, M. A. (2019): Inter-genus gene expression analysis in livestock fibroblasts using reference gene validation based upon a multi-species primer set. *PLoS One* **14**, e0221170.
- Nakamura, S., Yokota, D., Tan, L., Nagata, Y., Takemura, T., Hirano, I., Shigeno, K., Shibata, K., Fujisawa, S. and Ohnishi, K. (2012): Down-regulation of Thanatos-associated protein 11 by BCR-ABL promotes CML cell proliferation through c-Myc expression. *Int. J. Cancer* **130**, 1046–1059.
- Nuttinck, F., Reinaud, P., Tricoire, H., Vigneron, C., Peynot, N., Mialot, J. P., Mermillod P. and Charpigny, G. (2002): Cyclooxygenase-2 is expressed by cumulus cells during oocyte maturation in cattle. *Mol. Reprod. Dev.* **61**, 93–101.
- Nuttinck, F., Charpigny, G., Mermillod, P., Loosfelt, H., Meduri, G., Freret, S., Grimard, B. and Heyman, Y. (2004): Expression of components of the insulin-like growth factor system and gonadotropin receptors in bovine cumulus-oocyte complexes during oocyte maturation. *Domest. Anim. Endocrinol.* **27**, 179–195.
- O'Connor, T., Wilmut, I. and Taylor, J. (2013): Quantitative evaluation of reference genes for real-time PCR during *in vitro* maturation of ovine oocytes. *Reprod. Domest. Anim.* **48**, 477–483.
- Olson, E. N. (2006): Gene regulatory networks in the evolution and development of the heart. *Science* **313**, 1922–1927.
- Pfaffl, M. W., Horgan, G. W. and Dempfle, L. (2002): Relative expression software tool (REST) for groupwise comparison and statistical analysis of relative expression results in real-time PCR. *Nucleic Acids Res.* **30**, 1–10.
- Pfaffl, M. W., Tichopad, A., Prgomet, C. and Neuvians, T. P. (2004): Determination of stable housekeeping genes, differentially regulated target genes and sample integrity: BestKeeper-Excel-based tool using pair-wise correlations. *Biotechnol. Letters* **26**, 509–515.
- Rahl, P. B. and Young, R. A. (2014): MYC and transcription elongation. *Cold Spring Harb. Perspect. Med.* **4**, a020990.
- Richani, D. and Gilchrist, R. B. (2018): The epidermal growth factor network: role in oocyte growth, maturation and developmental competence. *Hum. Reprod. Update* **24**, 1–14.
- Richards, J. S. (2005): Ovulation: new factors that prepare the oocyte for fertilization. *Mol. Cell. Endocrinol.* **29**, 75–79.
- Russell, D. L., Gilchrist, R. B., Brown, H. M. and Thompson, J. G. (2016): Bidirectional communication between cumulus cells and the oocyte: old hands and new players? *Theriogenology* **86**, 62–68.
- Schoenfelder, M. and Einspanier, R. (2003): Expression of hyaluronan synthases and corresponding hyaluronan receptors is differentially regulated during oocyte maturation in cattle. *Biol. Reprod.* **69**, 269–277.
- Sears, R., Nuckolls, F., Haura, E., Taya, Y., Tamai, K. and Nevins, J. R. (2000): Multiple Ras-dependent phosphorylation pathways regulate Myc protein stability. *Genes Dev.* **14**, 2501–2514.
- Silva, L. R. O., Silva, M. D., Ferreira Neto, J. R. C., De Nardi, C. H., Chabregas, S. M., Burnquist, W. L., Kahl, G., Benko-Iseppon, A. M. and Kido, E. A. (2014): Validation of novel reference genes for reverse transcription quantitative real-time PCR in drought-stressed sugarcane. *Sci. World J.* **2014**, 357052.
- Silva, P. G. C., Moura, M. T., Silva, R. L. O., Nascimento, P. S., Silva, J. B., Ferreira-Silva, J. C., Cantanhêde, L. F., Chaves, M. S., Benko-Iseppon, A. M. and Oliveira, M. A. L. (2018): Temporal expression of pluripotency-associated transcription factors in sheep and cattle preimplantation embryos. *Zygote* **26**, 270–278.
- Silver, N., Best, S., Jiang, J. and Thein, S. L. (2006): Selection of housekeeping genes for gene expression studies in human reticulocytes using real-time PCR. *BMC Mol. Biol.* **7**, 1–9.
- Sirard, M. A., Desrosier, S. and Assidi, M. (2007): *In vivo* and *in vitro* effects of FSH on oocyte maturation and developmental competence. *Theriogenology* **68**, S71–S76.
- Szklarczyk, D., Gable, A. L., Nastou, K. C., Lyon, D., Kirsch, R., Pyysalo, S. and von Mering, C. (2021): The STRING database in 2021: customizable protein–protein networks, and functional characterization of user-uploaded gene/measurement sets. *Nucleic Acids Res.* **49**(D1), D605–D612.
- Taylor, S. C., Nadeau, K., Abbasi, M., Lachance, C., Nguyen, M. and Fenrich, J. (2019): The Ultimate qPCR experiment: producing publication quality, reproducible data the first time. *Trends Biotechnol.* **37**, 761–774.
- Vandesompele, J., De Preter, K., Pattyn, F., Poppe, B., Van Roy, N., De Paepe, A. and Speleman, F. (2002): Accurate normalization of real-time quantitative RT-PCR data by geometric averaging of multiple internal control genes. *Genome Biol.* **3**, Research 0034.
- Van Tol, H. T. A., Van Eijk, M. J. T., Mummery, C. L., Van Den Hurk, R. and Bevers, M. M. (1996): Influence of FSH and hCG on the resumption of meiosis of bovine oocytes surrounded by cumulus cells connected to membrana granulosa. *Mol. Reprod. Dev.* **45**, 218–224.
- Vinayagam, A., Stelzl, U., Foulle, R., Plassmann, S., Zenkner, M., Timm, J., Assmus, H. E., Andrade-Navarro, M. A. and Wanker, E. E. (2011): A directed protein interaction network for investigating intracellular signal transduction. *Sci. Signaling* **4**, rs8–rs8.
- Wang, Y. K., Li, X., Song, Z. Q. and Yang, C. X. (2017): Methods of RNA preparation affect mRNA abundance quantification of reference genes in pig maturing oocytes. *Reprod. Domest. Anim.* **52**, 722–730.
- Wang, Z., Ge, L., Wang, M. and Carr, B. I. (2006): Phosphorylation regulates Myc expression via prolonged activation of the mitogen-activated protein kinase pathway. *J. Cell. Physiol.* **208**, 133–140.
- Wei, S., Shen, X., Lai, L., Liang, H., Deng, Y., Gong, Z. and Che, T. (2018): FSH receptor binding inhibitor impacts K-Ras and



- c-Myc of ovarian cancer and signal pathway. *Oncotarget* **9**, 22498–22508.
- Xie, F., Xiao, P., Chen, D., Xu, L. and Zhang, B. (2012): miR-DeepFinder: a miRNA analysis tool for deep sequencing of plant small RNAs. *Plant Mol. Biol.* **80**, 75–84.
- Yang, J., Gong, Z., Shen, X., Bai, S., Bai, X. and Wei, S. (2019): FSH receptor binding inhibitor depresses carcinogenesis of ovarian cancer via decreasing levels of K-Ras, c-Myc and FSHR. *Anim. Biotechnol.* **28**, 1–8.
- Zhang, J., Zhang, H., Shi, H., Wang, F., Du, J., Wang, Y., Wei, Y., Xue, W., Li, D., Feng, Y., Yan, J., Gao, Y., Li, J. and Han, J. (2020): THAP11 Functions as a tumor suppressor in gastric cancer through regulating c-Myc signaling pathways. *BioMed Res. Int.* **2020**, 7838924.

